

Analysis of Parametric Oscillatory Instability in Signal Recycled LIGO Interferometer with Different Arms

S.E. Strigin and S.P. Vyatchanin

*Faculty of Physics, Moscow State University,
Moscow 119992, Russia,
e-mail: svyatchanin@phys.msu.su
(Dated: November 3, 2006)*

The basis of undesirable effect of parametric oscillatory instability in signal recycled LIGO interferometer is the excitation of the additional (Stokes) optical mode, with frequency ω_1 , and the mirror elastic mode, with frequency ω_m , when optical energy stored in the main mode, with frequency ω_0 , exceeds the certain threshold and the frequencies are related as $\omega_0 \simeq \omega_1 + \omega_m$. We analyze parametric instability in the general case when eigen frequencies of Fabry-Perot (FP) cavities in arms of interferometer are detuned from each other and show that parametric instability in this interferometer is relatively small due to small bandwidth of interferometer. We propose to “scan” the frequency range where parametric instability may take place varying the position of signal recycling mirror.

I. INTRODUCTION

The full scale terrestrial interferometric gravitational wave antennae LIGO are operating now and have sensitivity, expressed in terms of the metric perturbation amplitude, only 2 or 3 times worse than the planned level of $h \simeq 1 \times 10^{-21}$ [1, 2] (see current sensitivity curve in [3]). In Advanced LIGO (to be realized in approximately 2012), after the improvement of the isolation from noises in the mirrors of the 4 km long optical Fabry-Perot (FP) cavities and increasing the optical power circulating in the resonator up to $W \simeq 830$ kW the sensitivity is expected to reach the value of $h \simeq 1 \times 10^{-22}$ [4, 5].

In [6] we have analyzed the undesirable effect of parametric oscillatory instability in the FP cavity, which may cause a substantial decrease of the antennae sensitivity or even the antenna malfunction. This effect appears above the certain threshold of the optical power W_c circulating in the main mode, when the difference $\omega_0 - \omega_1$ between the frequency ω_0 of the main optical mode and the frequency ω_1 of the idle (Stokes) mode is close to the frequency ω_m of the mirror mechanical degree of freedom. The coupling between these three modes arises due to the ponderomotive pressure of light in the main and Stokes modes and the parametric action of mechanical oscillation on the optical modes. Above the critical value of light power W_c the amplitude of mechanical oscillation rises exponentially as well as optical power in the idle (Stokes) optical mode. However, E. D’Ambrosio and W. Kells have shown [7] that if in the same single dimensional model the anti-Stokes mode (with frequency $\omega_{1a} = \omega_0 + \omega_m$) is taken into account, then the effect of parametric instability will be substantially dumped or even excluded. In [8] it has been presented the analysis based on the model of power recycled LIGO interferometer and it was demonstrated that anti-Stokes mode could not completely suppress the effect of parametric oscillatory instability. As possible “cure” to avoid the parametric instability we have proposed to change the

mirror shape and introduce low noise damping [9]. D. Blair with collaborators proposed valuable idea to heat the test masses in order to vary curvature radii of mirrors in interferometer and hence to control detuning and decrease overlapping factor between optical and acoustic modes [10–12]. Recently, the instability produced by optical rigidity was observed in experiment [13]. Parametric instability was also observed in resonant bar detectors with microwave resonant readout [14].

It is interesting that the effect of parametric instability is important not only for large scale LIGO interferometer. K. Vahala with collaborators observed it for micro scale whispering gallery optical resonators [15, 16].

Recently we have proposed the detail analysis of parametric instability in signal recycled Advanced LIGO interferometer (i.e. with additional signal recycling (SR) mirror)[17], assuming that FP cavities in arms are optically identical. However, Bill Kells [18, 19] put attention that FP cavities in arms can have *different* eigen frequencies because curvature radii of mirrors may differ from each other by about several meters ($\simeq 0.1\%$). Indeed, for the frequencies of Hermite-Gauss modes in FP cavity with mirrors radii R_1, R_2 and length L between them we have formula [20]

$$\omega_{qmn} = \frac{\pi c}{L} \left(q + (m + n + 1) \frac{\phi}{\pi} \right), \quad (1.1)$$

$$\phi \equiv \arccos(\pm \sqrt{g_1 g_2}), \quad g_{1,2} = 1 - \frac{L}{R_{1,2}}. \quad (1.2)$$

Here $q = 0, 1, 2, \dots$ is longitudinal index, m, n are transversal indices, g_1, g_2 are g-factors, ϕ is Guoy phase. In formula for ϕ sign (+) applies if $g_1 > 0, g_2 > 0$, sign (–) applies if $g_1 < 0, g_2 < 0$, different signs (i.e. $g_1 g_2 < 0$) corresponds to unstable resonator.

For parameters planned in Advanced LIGO [5]

$$R_{1,2} = 2076 \pm 3 \text{ m}, \quad L = 4 \text{ km}, \quad (1.3)$$

$$g_{1,2} = g = -0.9265 \pm 3 \times 10^{-3}, \quad \phi \simeq 0.3858, \quad (1.4)$$

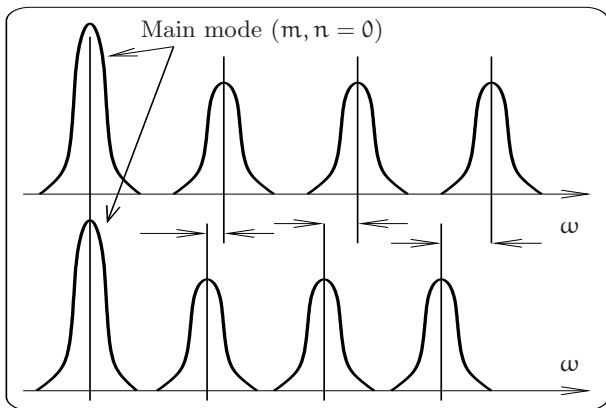


FIG. 1: Eigen modes of FP cavities in different arms. Main modes with indices $m = n = 0$ (shown by higher peaks) are tuned in resonance and other modes differ in FP cavities.

the frequencies of modes will differ by

$$\Delta f_{qmn} = \pm \frac{\Delta \omega_{qmn}}{2\pi} \simeq \pm (m + n + 1) 100 \text{ Hz}. \quad (1.5)$$

It is a large value if we remember that frequency range of Advanced LIGO sensitivity is planned between 50 and 500 Hz and relaxation rate of optical modes in interferometer — about 2 sec^{-1} . Recall that main modes of FP cavities in arms are tuned in resonance by feedback control system. Then additional modes (which can play role of Stokes modes) will be different as shown in Fig. 1. It means that we can not consider FP cavities in arms to be optically identical ones as in [17].

In this paper we analyze parametric instability in Advanced LIGO interferometer with detuned arms. We show that arms detuning provides shift of normal frequencies of whole interferometer, however, the probability of parametric instability does not differ considerably from the case of optically identical arms. It means that, on the one hand, the parametric instability in this interferometer can appear at low optical power (about several Watts) but, on the other hand, the probability that parametric instability condition will be fulfilled is small due to small relaxation rates of optical modes (about several Hz).

In section II we derive the parametric instability conditions in signal recycled LIGO interferometer with detuned arms, we discuss these results in section III. The details of calculations we present in Appendices.

II. SIGNAL RECYCLED INTERFEROMETER WITH DIFFERENT FP CAVITIES IN ARMS

We consider the LIGO interferometer with signal recycling (SR) and power recycling (PR) mirrors — see fig. 2. Simplifications are the following:

- We do not take into account optical losses and suspension noise in all mirrors.

- Eigen frequencies ω_1 and ω_2 of Stokes modes in FP cavities in arms slightly differ from mean frequency $\omega_s = (\omega_1 + \omega_2)/2$ by arms detuning $d \equiv (\omega_1 - \omega_2)/2$ so that $\omega_{1,2} = \omega_s \pm d$. For simplicity we assume that relaxation rates and transparencies of input mirrors are the same: $\gamma_1 = \gamma_2 = \gamma$, $T_1 = T_2 = T$.

- The distances between input FP mirrors and beam splitter and between beam splitter and PR, SR mirrors are short (about several meters) — hence we consider the phase advance of waves traveling between these mirrors as a constant and omit dependence on frequency (of these phases).

Interferometer is pumped via port F_5 .

A. FP cavities in arms

We introduce the mean amplitude and small fluctuational amplitude (denoting by small letters). For example for amplitude in FP cavity 1 this means: $F_{1in} = \mathcal{F}_0 + f_{1in}$, where mean field \mathcal{F}_0 corresponds to main mode with frequency ω_0 and fluctuational field f_{1in} — to Stokes mode with mean frequency ω_s . We start from formula (A10) in Appendix A:

$$f_{1in}(\Omega) = T_1 f_1(\Omega) + N_1 \mathcal{F}_0 \frac{T_1 2ikz_1^*(\Delta - \Omega)}{i\sqrt{T}}, \quad (2.1)$$

$$e_1(\Omega) = \mathcal{R}_1 f_1(\Omega) - N_1 \mathcal{F}_0 T_1 2ikz_1^*(\Delta - \Omega), \quad (2.2)$$

$$T_1 = \frac{2i\gamma}{\sqrt{T}(\gamma - i(\Omega - d))}, \quad \mathcal{R}_1 = \frac{\gamma + i(\Omega - d)}{\gamma - i(\Omega - d)}, \quad (2.3)$$

$$\Delta = \omega_0 - \omega_s - \omega_m, \quad (2.4)$$

$$\omega_s = \frac{\omega_1 + \omega_2}{2}, \quad d = \frac{\omega_2 - \omega_1}{2} \quad (2.5)$$

$$z_1(\Omega) \equiv x_1(\Omega) - y_1(\Omega), \quad \gamma = cT/4L,$$

$$f_{2in}(\Omega) = T_2 f_2(\Omega) + N_2 \mathcal{F}_0 \frac{T_2 2ikz_2^*(\Delta - \Omega)}{i\sqrt{T}}, \quad (2.6)$$

$$e_2(\Omega) = \mathcal{R}_2 f_2(\Omega) - N_2 \mathcal{F}_0 T_2 2ikz_2^*(\Delta - \Omega), \quad (2.7)$$

$$T_2 = \frac{2i\gamma}{\sqrt{T}(\gamma - i(\Omega + d))}, \quad \mathcal{R}_2 = \frac{\gamma + i(\Omega + d)}{\gamma - i(\Omega + d)}, \quad (2.8)$$

$$z_2(\Omega) \equiv x_2(\Omega) - y_2(\Omega), \quad (2.9)$$

$$E_1 = \mathcal{R}_1 F_1, \quad E_2 = \mathcal{R}_2 F_2, \quad \mathcal{R}_{1,2} = \mathcal{R}_{1,2}(\Omega = 0).$$

Here N_1 is dimensionless overlapping factor (A3), Δ is parametric instability (PI) detuning. We write down the formula in frequency domain, introducing slow amplitudes of mechanical displacement $\bar{z}_1(t) = z_1(t) e^{-i\omega_m t} + z_1^*(t) e^{i\omega_m t}$ and their Fourier transforms. In order to clarify the presenting formulas we have to write in details the last term in (2.1) as following:

$$\mathcal{F}_{1in} e^{-i(\omega_0 - \omega_1)t} \frac{T_1}{i\sqrt{T}_1} \times$$

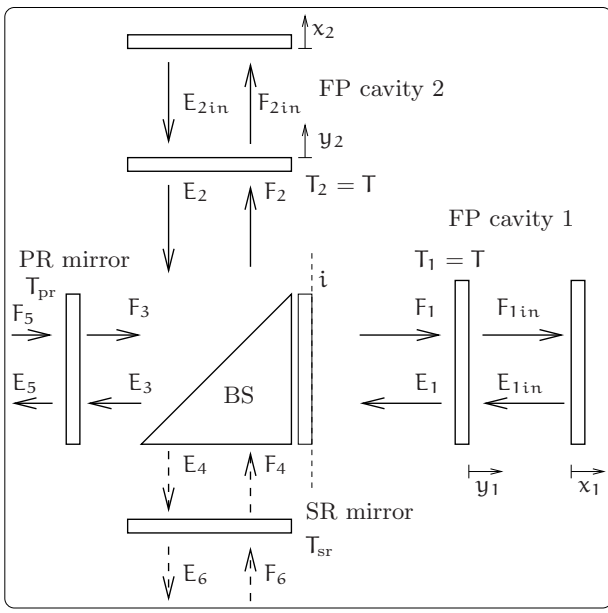


FIG. 2: Signal and power recycled LIGO interferometer. Here F_1 , E_1 are amplitudes on incur mirror of FP cavity 1 (and on plane (i)), F_2 , E_2 are amplitudes on incur mirror of FP cavity 2 and on beam splitter, F_3 , E_3 , F_4 , E_4 are amplitudes on beamsplitter.

$$\times 2ik \left(z(\Omega') e^{-i\omega_m - \Omega'} t + z_1^*(\Omega') e^{i(\omega_m + \Omega') t} \right).$$

We omit non-resonance term $\sim z(\Omega')$ and then we equate under exponent terms from the left and from the right in (2.1):

$$-i\Omega t = -i(\omega_0 - \omega_1)t + i(\omega_m + \Omega')t \rightarrow \Omega' = \Delta - \Omega$$

B. Beam Splitter (BS)

We consider that F_3 , E_3 and F_4 , E_4 are amplitudes on BS as it shown in Fig. 2. We assume that BS transparency is $T_{bs} = 1/2$ and the phase of wave due to traveling between FP cavity 2 and BS is $e^{i\phi_2} = 1$ and between FP cavity 1 and BS is $e^{i\phi_1} = i$. So we can imagine such plane (i) (see Fig. 2) that phase advance between BS and this plane is $e^{i\phi_1} = i$ and between this plane and input mirror of FP cavity 1 is fold to 2π . Then F_1 , E_1 are amplitudes on input mirror of FP cavity 1 (and on plane (i)), F_2 , E_2 are amplitudes on input mirror of FP cavity 2 and on BS:

$$F_1 = \frac{-F_3 - iF_4}{\sqrt{2}}, \quad F_2 = \frac{1}{\sqrt{2}}(-F_3 + iF_4), \quad (2.10)$$

$$F_3 = \frac{-F_1 - F_2}{\sqrt{2}}, \quad F_4 = \frac{i}{\sqrt{2}}(F_1 - F_2), \quad (2.11)$$

$$E_3 = \frac{-E_1 - E_2}{\sqrt{2}}, \quad E_4 = \frac{i(-E_1 + E_2)}{\sqrt{2}}. \quad (2.12)$$

C. Power Recycling and Signal Recycling Mirrors

On PR mirror we have (F_3 and E_3 are amplitudes on BS):

$$F_3 e^{-i\phi_{pr}} = i\sqrt{T_{pr}}F_5 - \sqrt{1 - T_{pr}}E_3 e^{i\phi_{pr}}, \quad (2.13)$$

$$E_5 = i\sqrt{T_{pr}}E_3 e^{i\phi_{pr}} - \sqrt{1 - T_{pr}}F_5, \quad (2.14)$$

$$\phi_{pr} = (\omega_1 + \Delta_{pr} + \Omega)l_{pr}/c. \quad (2.15)$$

We assume that PR cavity in resonance: $\exp(i\phi_{pr}) = i$ and we assume that ϕ_{pr} does not depend on frequency Ω due to shortness of PR cavity ($l_{pr} \ll L$). So we have:

$$F_3 = \sqrt{1 - T_{pr}}E_3 - \sqrt{T_{pr}}F_5, \quad (2.16)$$

$$E_5 = -\sqrt{T_{pr}}E_3 - \sqrt{1 - T_{pr}}F_5. \quad (2.17)$$

On SR mirror we have (F_4 and E_4 are amplitudes on BS):

$$F_4 e^{-i\phi} = i\sqrt{T_{sr}}F_6 - \sqrt{1 - T_{sr}}E_4 e^{i\phi}, \quad (2.18)$$

$$E_6 = i\sqrt{T_{sr}}E_4 e^{i\phi} - \sqrt{1 - T_{sr}}F_6. \quad (2.19)$$

We assume that SR cavity is not in resonance (i.e. $\phi = (\omega_1 + \Omega)l_{sr}/c$ is an arbitrary multiplier) and we assume that ϕ does not depend on frequency Ω due to shortness of SR cavity ($l_{sr} \ll L$).

D. Equations for fields inside cavities

In order to find the equations for fields f_{1in} , f_{2in} inside cavities we substitute (2.11, 2.12) into set (2.16, 2.18) and then using Eqs. (2.1, 2.2, 2.6, 2.7) we obtain equations:

$$\begin{aligned} f_{1in}(\gamma_+ - i(\Omega - d)) + f_{2in}(\gamma_+ - i(\Omega + d)) &= \mathcal{Z}_+, \\ f_{1in}(\Gamma_- - i(\Omega - d)) - f_{2in}(\Gamma_- - i(\Omega + d)) &= \mathcal{Z}_-, \\ \mathcal{Z}_1 &= \frac{icN_1\mathcal{F}_0 kz_1^*}{L}, \quad \mathcal{Z}_2 = \frac{icN_1\mathcal{F}_0 kz_2^*}{L}, \\ \gamma_+ &= \gamma \frac{1 - \sqrt{1 - T_{pr}}}{1 + \sqrt{1 - T_{pr}}}, \quad \mathcal{Z}_\pm = \mathcal{Z}_1 \pm \mathcal{Z}_2, \quad (2.20) \\ \Gamma_- &\equiv \gamma_- - i\delta = \gamma \frac{1 - e^{2i\phi}\sqrt{1 - T_{sr}}}{1 + e^{2i\phi}\sqrt{1 - T_{sr}}}. \quad (2.21) \end{aligned}$$

Here values γ_+ , Γ_- have simple physical sense: γ_+ (γ_-) is a relaxation rate of symmetrical (anti-symmetrical) mode in interferometers with non-detuned arms (i.e. $d = 0$) [17] and δ is a SR detuning of antisymmetric mode depending on SR mirror position. Summing and subtracting these equations we obtain:

$$f_{1in}(g_+ - i(\Omega - d)) + f_{2in}g_- = \mathcal{Z}_1, \quad (2.22)$$

$$f_{1in}g_- + f_{2in}(g_+ - i(\Omega + d)) = \mathcal{Z}_2, \quad (2.23)$$

$$g_\pm = \frac{\gamma_+ \pm \Gamma_-}{2} = \frac{\gamma_+ \pm \gamma_- \mp i\delta}{2}. \quad (2.24)$$

E. Ponderomotive forces

We have to add equation with ponderomotive force (see Appendix A, Eqs. (A13)):

$$\dot{Z}_1 + \gamma_m Z_1 = 2Q f_{in1}(t) e^{i\Delta t}, \quad (2.25)$$

$$\dot{Z}_2 + \gamma_m Z_2 = 2Q f_{2in}(t) e^{i\Delta t}, \quad (2.26)$$

$$2Q = \frac{2\omega_1 |N_1|^2 |\mathcal{F}_0|^2}{mc\mu\omega_m L}. \quad (2.27)$$

F. Normal modes

We see that equations set (2.22,2.23) describe coupled oscillators and, hence, we can introduce normal modes (with complex amplitudes ξ , η) for interferometer with detuned arms. It allows us to rewrite equations set (2.22, 2.23) and equations (2.25,2.26) in time domain as following (see details in Appendix B):

$$(1 + \varkappa^2) (\partial_t - \lambda_1) \xi = z_\xi e^{-i\Delta t}, \quad (2.28)$$

$$\dot{z}_\xi + \gamma_m z_\xi = 2Q (1 + \varkappa^2) \xi(t) e^{i\Delta t} \quad (2.29)$$

$$(1 + \varkappa^2) (\partial_t - \lambda_2) \eta = z_\eta e^{-i\Delta t}, \quad (2.30)$$

$$\dot{z}_\eta + \gamma_m z_\eta = 2Q (1 + \varkappa^2) \eta(t) e^{i\Delta t}, \quad (2.31)$$

$$\xi = \frac{f_{1in} - \varkappa f_{2in}}{1 + \varkappa^2}, \quad \eta = \frac{\varkappa f_{1in} + f_{2in}}{1 + \varkappa^2}, \quad (2.32)$$

$$z_\xi = Z_1 - \varkappa Z_2, \quad z_\eta = \varkappa Z_1 + Z_2, \quad (2.33)$$

$$\lambda_{1,2} = -g_+ \pm \sqrt{g_-^2 - d^2}, \quad \varkappa = \frac{\sqrt{g_-^2 - d^2} + id}{g_-}. \quad (2.34)$$

We obtain two separate pairs of equations as for the case of non-detuned arms. Note that in case $d \rightarrow 0$ mode ξ transforms into anti-symmetrical mode (i.e. $\xi \rightarrow (f_{1in} - f_{2in})/2$, $z_\xi \rightarrow Z_1 - Z_2$) and mode η — into symmetrical mode (i.e. $\eta \rightarrow (f_{1in} + f_{2in})/2$, $z_\eta \rightarrow Z_1 + Z_2$).

For the most likely case we have strong inequality $|\gamma_+ - \gamma_-| \ll \delta$ (relaxation rates γ_\pm are in range $1 \dots 10 \text{ s}^{-1}$ and SR detuning δ introduced by SR mirror position is about 10^3 s^{-1}) and we can use approximation for (2.34):

$$\lambda_{1,2} \simeq \left(-\frac{\gamma_+ + \gamma_-}{2} \pm \frac{\delta(\gamma_+ - \gamma_-)}{2D} \right) + i \left(\frac{\delta}{2} \pm D \right), \quad (2.35)$$

$$\varkappa \simeq \frac{2(d + D)}{\delta}, \quad D = \sqrt{d^2 + \left(\frac{\delta}{2} \right)^2}. \quad (2.36)$$

For elastically identical mirrors (i.e. when all mirrors have the same masses and eigen frequencies) we can analyze two pairs (2.28, 2.29) and (2.30, 2.31) separately. For example, for the equations set (2.28, 2.29) we can obtain

characteristic equation (presenting $\xi = \xi e^{\lambda t - i\Delta t}$, $z_\xi = z_\xi e^{\lambda t}$)

$$2Q = (\lambda - i\Delta - \lambda_1)(\lambda + \gamma_m). \quad (2.37)$$

Estimates in Appendix C demonstrate the inequality:

$$\gamma_m \ll \gamma_+, \gamma_- \quad (2.38)$$

We are interested in root, which is close to relaxation rate of elastic mode: $|\lambda| \sim \gamma_m$. Hence, using (2.38) we can approximate characteristic equation (2.37) putting $\lambda = 0$ in all brackets, where γ_+ , γ_- (or λ_1) exist:

$$\lambda \simeq -\gamma_m - \frac{2Q}{i\Delta + \lambda_1} \quad (2.39)$$

Parametric instability condition corresponds to $\text{Re}(\lambda) < 0$:

$$\frac{2Q}{\gamma_m} \times \frac{-\text{Re}(\lambda_1)}{[\text{Re}(\lambda_1)]^2 + [\Delta + \text{Im}(\lambda_1)]^2} \geq 1 \quad (2.40)$$

For elastically different mirrors when frequencies of elastic modes do not coincide we can take into account displacement of only one mirror, for example, displacement x_1 of end mirror FP cavity 1, and we introduce $\mathcal{X}_1 = icN_1 \mathcal{F}_0 k x_1^* / L$. In this case set (2.28, 2.30, 2.25) transforms as following:

$$(1 + \varkappa^2) (\partial_t - \lambda_1) \xi = \mathcal{X}_1 e^{-i\Delta t}, \quad (2.41)$$

$$(1 + \varkappa^2) (\partial_t - \lambda_2) \eta = \varkappa \mathcal{X}_1 e^{-i\Delta t}, \quad (2.42)$$

$$\dot{\mathcal{X}}_1 + \gamma_m \mathcal{X}_1 = Q (\xi(t) + \varkappa \eta(t)) e^{i\Delta t} \quad (2.43)$$

Going from (2.25) to (2.43) we take into account that effective force has to be two times smaller (because it acts on one mirror only). Presenting $\xi = \xi e^{\lambda t - i\Delta t}$, $\eta = \eta e^{\lambda t - i\Delta t}$, $\mathcal{X}_1 i = \mathcal{X}_1 e^{\lambda t}$ we obtain characteristic equation: in form similar to the case ($d = 0$) [17]:

$$\lambda + \gamma_m = \frac{Q}{(1 + \varkappa^2)} \left(\frac{1}{\lambda - i\Delta - \lambda_1} + \frac{\varkappa^2}{\lambda - i\Delta - \lambda_2} \right) \quad (2.44)$$

The using condition (2.38) we can obtain parametric instability condition:

$$\frac{Q}{(1 + \varkappa^2)\gamma_m} \left(\frac{-\text{Re}(\lambda_1)}{[\text{Re}(\lambda_1)]^2 + [\Delta + \text{Im}(\lambda_1)]^2} + \frac{-\varkappa^2 \text{Re}(\lambda_2)}{[\text{Re}(\lambda_2)]^2 + [\Delta + \text{Im}(\lambda_2)]^2} \right) \geq 1. \quad (2.45)$$

III. DISCUSSION AND CONCLUSION

For our discussion we use the following scale of relaxations rates (see Appendix C): the relaxation rate of

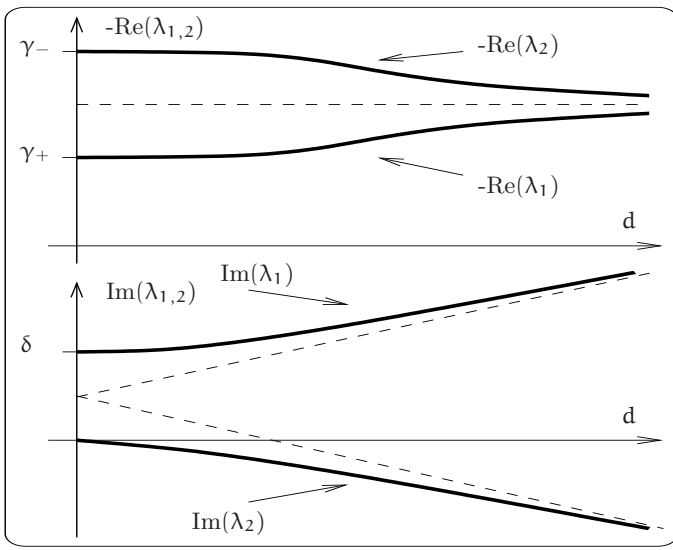


FIG. 3: Dependences of real (top) and imaginary (bottom) parts of $\lambda_{1,2}$

elastic mode $\gamma_m \simeq 6 \times (10^{-4} \div 10^{-2}) \text{ sec}^{-1}$, the relaxation rates of symmetric and anti-symmetric modes $\gamma_{0+} \simeq 1.5 \text{ sec}^{-1}$, $\gamma_{0-} \geq 2 \text{ sec}^{-1}$, and the relaxation rate of a single FP cavity in arm $\gamma \simeq 100 \text{ sec}^{-1}$.

We see that parametric instability conditions for Advanced LIGO interferometer with detuned arms obviously relates with interferometer with non-detuned arms considered in [17]. Indeed, conditions (2.40, 2.45) transform into conditions (2.16, 2.30) in [17] correspondingly if we make substitutions:

$$\lambda_1 \rightarrow -\gamma_- + i\delta, \quad \lambda_2 \rightarrow -\gamma_+ \quad (3.1)$$

Hence, the dependence of eigen values $\lambda_{1,2}$ on arms detuning d provides the complete information we need.

The plots of Fig. 3 show this dependence qualitatively. We see that real parts of $\lambda_{1,2}$, described relaxation rate of normal modes, do not change dramatically. Therefore, we can conclude that crucial dependence on PI detuning Δ is valid also for Advanced LIGO interferometer with detuned arms, i.e. parametric instability takes place when PI detuning is relatively small: $|\Delta| < \gamma_{0+}$, $\gamma_{0-} \simeq 2 \text{ sec}^{-1}$.

From bottom plot in Fig. 3 we see that arms detuning d may change the frequencies of normal modes considerably. However, it does not change the density of optical modes and, hence, does not change the chance to fall into trap of parametric instability.

On the one hand, in case of parametric resonance (when total detuning is small: $\Delta + \text{Im}\lambda_{1,2} \ll \gamma_+, \gamma_-$) the parametric instability in a signal recycled interferometer takes place at relatively low value of optical power. For example, if $|\Delta + \text{Im}(\lambda_1)| \ll \gamma_{0+}$, γ_- and $|\Delta + \text{Im}(\lambda_2)| \gg \gamma_{0+}$, γ_- one can obtain from Eq. (2.45) that the parametric instability will take place even at small power $W_c \simeq 5 \text{ W}$ (!) circulating in arms (if

$\omega_m = 10^5 \text{ sec}^{-1}$, $\gamma_m = 6 \times 10^{-4} \text{ sec}^{-1}$, $|N_1|^2/\mu \simeq 1$). On the other hand, there is a small chance that such small PI detuning will take place and for large PI detuning ($|\Delta + \text{Im}(\lambda_1)| > \gamma_{0+}$, γ_-) the realization of parametric instability requires dramatically larger optical power: $W_c \sim (\Delta + \text{Im}(\lambda_1))^2/\gamma_{0+}^2$. For example, if detuning is about 1 kHz ($|\Delta + \text{Im}(\lambda_1)| \simeq 6 \times 10^3 \text{ sec}^{-1}$) and other parameters are the same one can obtain $W_c \simeq 10^8 \text{ W}$ (!). For the same reason the possibility that the presence of anti-Stokes mode can depress the parametric instability is small enough especially for such PI detuning. Therefore, we did not consider the anti-Stokes mode in our analysis.

Our consideration can be generalized for the case of mirrors with losses for the same reason as in [17].

The most reliable method to avoid the parametric instability is the *direct experimental* test. For signal recycled interferometer we can vary SR and arms detunings (δ and d) to investigate the parametric instability experimentally *in situ*. One can vary SR detuning δ by displacement of the SR mirror position [17] and arms detuning d by variation curvature radius of mirrors though its inhomogeneous heating. It will allow to scan relatively wide spectral range to find dangerous (from the point of view of parametric instability) places. This scanning combined with the detailed knowledge about the elastic modes (it can be obtained *in situ* in separate experiments before the test masses are placed into the interferometer) will provide us with very valuable information to avoid the parametric instability.

Acknowledgments

We are grateful to Vladimir Braginsky, Bill Kells, Adrian Melissinos and David Ottaway for fruitful discussions. This work was supported by LIGO team from Caltech and in part by NSF and Caltech grant PHY-0353775, by the Russian Agency of Industry and Science, contracts No. 5178.2006.2 and 02.445.11.7423.

Appendix A: FP cavity with two movable mirrors

We consider two optical fields in cavity with moveable mirrors (Fig. 4)—with constant amplitude in main mode $\mathcal{F}_{0\text{in}}$ with frequency ω_0 and fluctuational field $f_{1\text{in}}$ in Stokes mode with frequency ω_1 . Capital letters denote mean complex amplitudes, small letters — fluctuational and signal components. Transmittivity and reflectivity of input mirror is T and R correspondingly ($T + R = 1$). We assume $T \ll 1$. Back mirror is completely reflecting.

Main mode is in resonance with pump.

Now we can write down equation for elastic oscillations with amplitude \mathbf{x} :

$$\rho \sum_{\ell} \bar{\mathbf{u}}_{\ell} (\ddot{\mathbf{x}}_{\ell} + 2\gamma_{\mathbf{m}}^{(\ell)} \dot{\mathbf{x}}_{\ell} + (\omega_{\mathbf{m}}^{(\ell)})^2 \mathbf{x}_{\ell}) = \bar{\mathbf{n}}_{\mathbf{x}} \mathbf{P}(\bar{\mathbf{r}}_{\perp}) \delta(r_{\parallel} - r_{\parallel}^0)$$

Here ρ is density of mirror, sum is taken over the complete set of elastic modes (spatial displacements vectors $\bar{\mathbf{u}}_{\ell}$ are orthogonal to each other), $\bar{\mathbf{n}}_{\perp}$ is unit normal to mirror's surface, r_{\parallel} is longitudinal coordinate of points inside body of mirror, coordinate r_{\parallel}^0 corresponds to face surface of mirror. Multiplying this equation by spatial distribution vector $\bar{\mathbf{u}}^*$ of our elastic mode and integrating over volume V of mirror body one can obtain:

$$\ddot{\mathbf{x}} + 2\gamma_{\mathbf{m}} \dot{\mathbf{x}} + \omega_{\mathbf{m}}^2 \mathbf{x} = \frac{2(N_1^* \mathcal{F}_{0\text{in}}^* f_{\text{in}1}(t) e^{i(\omega_0 - \omega_1)t} + \text{c.c.})}{\text{cm}\mu},$$

$$\mu = \frac{1}{V} \int |\bar{\mathbf{u}}(\bar{\mathbf{r}})|^2 d\bar{\mathbf{r}}, \quad (\text{A11})$$

where $\mathbf{m} = \rho V$ is mirror's mass.

Presenting $\mathbf{x} \Rightarrow \mathbf{x} e^{-i\omega_{\mathbf{m}} t} + \mathbf{x}^* e^{i\omega_{\mathbf{m}} t}$ (introduction of slow amplitudes) we obtain equation for amplitude \mathbf{x}^* :

$$\dot{\mathbf{x}}^* + \gamma_{\mathbf{m}} \mathbf{x}^* = \frac{N_1^*}{i\text{cm}\mu\omega_{\mathbf{m}}} \mathcal{F}_{1\text{in}}^* f_{\text{in}1}(t) e^{i\Delta t} \quad (\text{A12})$$

And for the coordinate $\mathbf{z} = \mathbf{x} - \mathbf{y}$ we finally obtain (mirrors are elastically identical):

$$\dot{\mathbf{z}}^* + \gamma_{\mathbf{m}} \mathbf{z}^* = \frac{2N_1^*}{i\text{cm}\mu\omega_{\mathbf{m}}} \mathcal{F}_{1\text{in}}^* f_{\text{in}1}(t) e^{i\Delta t} \quad (\text{A13})$$

Appendix B: Normal modes in LIGO interferometer with detuned arms

We have the following set of equation for fields $f_{1\text{in}}$, $f_{2\text{in}}$ inside arms:

$$(\partial_t + i\mathbf{d} + g_+) f_{1\text{in}} + g_- f_{2\text{in}} = \mathcal{Z}_1 e^{-i\Delta t} = \zeta_1, \quad (\text{B1})$$

$$g_- f_{1\text{in}} + (\partial_t - i\mathbf{d} + g_+) f_{2\text{in}} = \mathcal{Z}_2 e^{-i\Delta t} = \zeta_2, \quad (\text{B2})$$

To find normal mode we should solve this set with zero right parts. The characteristic equation of such set and its solution is the following:

$$(\lambda + i\mathbf{d} + g_+) (\lambda - i\mathbf{d} + g_+) - g_-^2 = 0, \quad (\text{B3})$$

$$\lambda_{1,2} = -g_+ \pm \sqrt{g_-^2 - d^2} \equiv$$

$$\equiv -\frac{\gamma_+ + \gamma_- - i\delta}{2} \pm \sqrt{\left(\frac{\gamma_+ - \gamma_- + i\delta}{2}\right)^2 - d^2} \quad (\text{B4})$$

In case of small relaxation (i.e. $\gamma_+, \gamma_- \rightarrow 0$) we have usual formula for coupled oscillators $\lambda_{1,2} \simeq i(\delta/2 \pm \sqrt{(\delta/2)^2 + d^2})$. To find normal modes we present

$$f_{1\text{in}} = A e^{\lambda_1 t} + \varkappa_1 B e^{\lambda_2 t}, \quad f_{2\text{in}} = \varkappa_2 A e^{\lambda_1 t} + B e^{\lambda_2 t}. \quad (\text{B5})$$

Substituting them into Eqs. (B1, B2) with zero right parts we obtain coefficients \varkappa_1, \varkappa_2 :

$$\varkappa_1 = -\frac{\lambda_2 - i\mathbf{d} + g_+}{g_-} = \frac{-g_-}{\lambda_2 + i\mathbf{d} + g_+} = \frac{\sqrt{g_-^2 - d^2 + i\mathbf{d}}}{g_-},$$

$$\varkappa_2 = -\frac{\lambda_1 + i\mathbf{d} + g_+}{g_-} = \frac{-g_-}{\lambda_1 - i\mathbf{d} + g_+} = -\frac{\sqrt{g_-^2 - d^2 + i\mathbf{d}}}{g_-}.$$

Below we denote: $\varkappa_1 = \varkappa$, $\varkappa_2 = -\varkappa$. Now we can introduce normal coordinates ξ, η and substitute into (B1, B2):

$$f_{1\text{in}} = \xi + \varkappa\eta, \quad f_{2\text{in}} = -\varkappa\xi + \eta, \quad (\text{B6})$$

$$(\partial_t - \lambda_1) \xi + \varkappa (\partial_t - \lambda_2) \eta = \zeta_1, \quad (\text{B7})$$

$$-\varkappa (\partial_t - \lambda_1) \xi + (\partial_t - \lambda_2) \eta = \zeta_2, \quad (\text{B8})$$

$$\xi = \frac{f_{1\text{in}} - \varkappa f_{2\text{in}}}{1 + \varkappa^2}, \quad \eta = \frac{\varkappa f_{1\text{in}} + f_{2\text{in}}}{1 + \varkappa^2}. \quad (\text{B9})$$

Now one can obtain separate equations for normal coordinates:

$$(\text{B7}) - \varkappa \times (\text{B8}): \quad (1 + \varkappa^2) (\partial_t - \lambda_1) \xi = \zeta_1 - \varkappa \zeta_2, \quad (\text{B10})$$

$$\varkappa \times (\text{B7}) + (\text{B8}): \quad (1 + \varkappa^2) (\partial_t - \lambda_2) \eta = \zeta_2 + \varkappa \zeta_1 \quad (\text{B11})$$

For the simple for analysis case is $|\gamma_+ - \gamma_-| \ll \delta$ one can expand into series formula (B4) for $\lambda_{1,2}$:

$$\lambda_{1,2} \simeq \left(-\frac{\gamma_+ + \gamma_-}{2} \pm \frac{\delta(\gamma_+ - \gamma_-)}{2D} \right) + i \left(\frac{\delta}{2} \pm D \right), \quad (\text{B12})$$

$$\varkappa \simeq \frac{2(d+D)}{\delta}, \quad D = \sqrt{d^2 + \left(\frac{\delta}{2}\right)^2}. \quad (\text{B13})$$

The case of small detuning $d \rightarrow 0$ corresponds to

$$\lambda_1 = -g_+ + \sqrt{g_-^2 - d^2} \rightarrow -\Gamma_-, \quad (\text{B14})$$

$$\lambda_2 = -g_+ - \sqrt{g_-^2 - d^2} \rightarrow -\gamma_+, \quad (\text{B15})$$

$$\varkappa = \frac{\sqrt{g_-^2 - d^2 + i\mathbf{d}}}{g_-} \rightarrow 1, \quad (\text{B16})$$

$$f_{1\text{in}} = \xi + \varkappa\eta \rightarrow \xi + \eta, \quad (\text{B17})$$

$$f_{2\text{in}} = -\varkappa\xi + \eta \rightarrow \eta - \xi, \quad (\text{B18})$$

$$\xi = \frac{f_{1\text{in}} - \varkappa f_{2\text{in}}}{1 + \varkappa^2} \rightarrow \frac{f_{1\text{in}} - f_{2\text{in}}}{2}, \quad (\text{B19})$$

$$\eta = \frac{\varkappa f_{1\text{in}} + f_{2\text{in}}}{1 + \varkappa^2} \rightarrow \frac{f_{1\text{in}} + f_{2\text{in}}}{2}. \quad (\text{B20})$$

We used the parameters planned for Advanced LIGO [5]:

$$\begin{aligned} \omega_0 \simeq \omega_1 &\simeq 2 \times 10^{15} \text{ sec}^{-1}, & L &= 4 \times 10^5 \text{ cm}, \\ m &= 40 \text{ kg}, & W &= 830 \text{ kW}, \\ T &= 5 \times 10^{-3}, & T_{\text{pr}} &= 6 \times 10^{-2}, \\ \gamma &\simeq 94 \text{ sec}^{-1}, & \gamma_{0+} &\simeq 1.5 \text{ sec}^{-1}, \\ T_{\text{sr}} &= 7 \times 10^{-2}. \end{aligned}$$

We also assume that FP mirrors are fabricated from fused silica with angle of structural losses $\phi = 1.2 \times 10^{-8}$ and for elastic modes frequencies $\omega_m = 10^5 \div 10^7 \text{ sec}^{-1}$ we estimate relaxation rate γ_m of elastic modes by formula:

$$\gamma_m = \omega_m \phi / 2 \simeq 6 \times (10^{-4} \div 10^{-2}) \text{ sec}^{-1}.$$

- [1] A. Abramovici *et al.*, *Science* **256**, 325 (1992).
 [2] A. Abramovici *et al.*, *Physics Letters A* **218**, 157 (1996).
 [3] LIGO technical document G060052-00-E; current sensitivity curves are available on http://www.ligo.caltech.edu/lazz/distribution/LSC_Data/.
 [4] Advanced LIGO System Design (LIGO-T010075-00-D), Advanced LIGO System requirements (LIGO-G010242-00), available in <http://www.ligo.caltech.edu>.
 [5] <http://www.ligo.caltech.edu/~ligo2/scripts/12refdes.htm>
 [6] V. B. Braginsky, S. E. Strigin, and S. P. Vyatchanin, *Physics Letters A* **287**, 331 (2001); gr-qc/0107079.
 [7] E. D'Ambrosio and W. Kells, *Physics Letter A* **299**, 326 (2002). LIGO-T020008-00-D, available in <http://www.ligo.caltech.edu>.
 [8] V. B. Braginsky, S. E. Strigin and S. P. Vyatchanin, *Physics Letters A* **305**, 111 (2002).
 [9] V. B. Braginsky and S. P. Vyatchanin, *Physics Letters A* **293**, 228 (2002).
 [10] C. Zhao, L. Ju, J. Degallaix, S. Gras, and D. G. Blair, *Phys. Rev. Lett.* **94**, 121102 (2005).
 [11] L. Ju, S. Gras, C. Zhao, J. Degallaix and D. G. Blair, *Phys. Lett. A* **354**, 360 (2006).
 [12] L. Ju, C. Zhao, S. Gras, J. Degallaix, D. G. Blair, J. Munch and D. H. Reitze, *Phys. Lett. A*, accepted (2006).
 [13] T. Corbitt, D. Ottaway, E. Innerhofer, J. Pelc, and N. Mavalvala *Phys. Rev. A* **74**, 021802 (2006).
 [14] B.S. Sheard, M.B. Gray, C.M. Mow-Lowry, D.E. McClelland, S.E. Whitcomb *Phys. Rev. A* **69**, 051801 (2004)
 [15] T. J. Kippenberg, H. Rokhsari, T. Carmon, A. Scherer, and K. J. Vahala, *Phys. Rev. Lett.* **95**, 033901, July 2005.
 [16] H. Rokhsari, T. J. Kippenberg, T. Carmon, and K. J. Vahala, *Optics express* **13**, 5293 (2005).
 [17] A.G. Gurkovsky, S.E. Strigin and S. P. Vyatchanin, accepted to *Physics Letters A*; arXive: gr-qc/0608007.
 [18] W.P. Kells, LIGO document T060159-00-D, available in <http://www.ligo.caltech.edu>.
 [19] W.P. Kells, LIGO document G050578-00-I, available in <http://www.ligo.caltech.edu>.
 [20] A.E. Siegman, *Lasers*, University Science Book, 1986.